Smith, J. V. (1970). *Lithos*, 3, 145–160.

Smith, J. V. (1974). *Feldspar Minerals*, Vol. 1, pp. 33–54, 208–228. Heidelberg: Springer-Verlag.

Smith, J. V. & Brown, W. L. (1988). *Feldspar Minerals*, Vol. 1, pp. 50–84, 127–129, 224–248, 416–436, 461–477. Heidelberg: Springer-Verlag.

Smith, K. L., McLaren, A. C. & O'Donnell, R. G. (1987). *Can. J. Earth Sci.* 24, 528–543.

Su, S. C., Bloss, F. D., Ribbe, P. H. & Stewart, D. B. (1984). *Am. Mineral.* 69, 440–448.

Wright, T. L. & Stewart, D. B. (1968). *Am. Mineral.* 53, 38–87.

Xu, H. (1993). PhD dissertation, Johns Hopkins Univ., Baltimore, USA.

Yund, R. A. (1983). *Feldspar Mineralogy, Reviews in Mineralogy*, Vol. 2, edited by P. H. Ribbe, pp. 177–202. Washington, DC: Mineralogical Society of America.

The Vertex Contribution to the Kirste–Porod Term

By Salvino Ciccariello

Dipartimento di Fisica 'G. Galilei' and Sezione INFM, via Marzolo 8, I-35131 Padova, Italy

and Roger Sobry

Laboratory of Experimental Physics, Institut of Physics B5, University of Liège, Sart Tilman, B-4000 Liège, Belgium

Abstract

It is shown that, close to the origin, the correlation function [$\gamma(r)$] of any N-component sample with interfaces made up of planar facets is always a third-degree polynomial in r. Hence, the only monotonically decreasing terms present in the asymptotic expansion of the relevant small-angle scattered intensity are the Porod [$-2\gamma'(0^+)/h^4$] and the Kirste–Porod [$4\gamma^{(3)}(0^+)/h^6$] contributions. The latter contribution is non-zero owing to the contributions arising from each vertex of the interphase surfaces. The general vertex contribution is evaluated in closed form and the $\gamma^{(3)}(0^+)$ values relevant to the regular polyhedra are reported.

I. Introduction

In the theory of small-angle scattering (SAS), samples are generally modelled as consisting of N homogeneous phases, each characterized by a constant electron or scattering-length-density value n_i and by the occupied sample subregion $\mathbf{V}_i$, $i = 1, ..., N$. The standard normalized scattered intensity $I(\mathbf{h})$ (Porod, 1982) is the Fourier transform of $\gamma(\mathbf{r})$, the so-called sample correlation function (CF). For isotropic samples, these quantities depend, respectively, only on h and r and are related by

$$I(h) = (4\pi V\langle\eta^2\rangle/h)\int_0^\infty r\gamma(r)\sin(hr)dr, \quad (1.1)$$

where*

$$\gamma(r) = 1 - \sum_{1 \le i < j \le N}[(n_i - n_j)^2/\langle\eta^2\rangle]P_{ij}(r), \quad (1.2)$$

$$P_{ij}(r) \equiv (1/4\pi V)\int d\hat\omega \int_{R^3} dv'\rho_i(\mathbf{r}')\rho_j(\mathbf{r}' + r\hat\omega), \quad (1.3)$$

$$\langle\eta^2\rangle = \sum_{1 \le i \le N}(n_i - \langle n\rangle)^2\phi_i$$

$$= \sum_{1 \le i < j \le N}(n_i - n_j)^2\phi_i\phi_j. \quad (1.4)$$

It should be noted that (1.2) and (1.3) do not require that interfaces are convex and that the sample is dilute. However, when the conditions are fulfilled, the second derivative of $\gamma(r)$, denoted $\gamma^{(2)}(r)$ or $\gamma''(r)$, coincides with Porod's intersect distribution function. According to a general theorem on Fourier transforms (Erdélyi, 1956), the behaviour of $I(h)$ at large h is related to the behaviour of the $\gamma(r)$ derivatives [$\gamma^{(n)}(r)$, $n = 1, 2, ...$] around the origin and around those r values, denoted δ_l ($l = 1, ..., M$),

---

* The meanings of the symbols involved in these equations are as follows: $h \equiv (4\pi/\lambda)\sin(\theta/2)$ with θ and λ respectively denoting the scattering angle and the beam-particle wavelength; V is the sample volume; $\phi_i \equiv V_i/V$ is the volume fraction of the ith phase; $\rho_i(\mathbf{r})$ is defined as being equal to unity when the tip of the position vector $\mathbf{r}$ falls inside region V_i and equal to zero elsewhere, and $\hat\omega$ is a unit vector that can assume all possible orientations. The bold capital symbols V and V_i should not be confused with vectors, which are always denoted by bold small capitals or, when they are unit vectors, by greek letters with carets.

where the $\gamma^{(n)}(r)$'s become singular. More precisely, the Erdélyi theorem requires that, as $r \to \delta_l^{\mp}$, $\gamma(r)$ behaves as $\mathscr{C}_l^{\pm}|r - \delta_l|^{1+\alpha_l}$ or as $\mathscr{C}_l^{\pm}|r - \delta_l|^{1+\alpha_l} \times \ln(|r - \delta_l|)$ (Jones & Kline, 1958), with $\alpha_l \geq 0$. Under these conditions, from (1.1), it asymptotically results that (Wu & Schmidt, 1974)

$$i(h) \equiv [I(h)/4\pi V\langle \eta^2 \rangle]$$

$$\approx \sum_l \mathscr{C}_l \cos(h\delta_l + \varphi_l)/h^{4+\alpha_l}, \qquad (1.5)$$

where $\mathscr{C}_l$ and φ_l are simply related to $\mathscr{C}_l^+$ and $\mathscr{C}_l^-$. Equation (1.5) shows that the monotonically decreasing terms are related to the behaviour of the CF derivatives at the origin (i.e. $\delta_l = 0$), while the damped oscillatory ones depend on the CF derivative behaviours around the non-null δ_l's. Showing that sample correlation functions have singular behaviours and relating the $\mathscr{C}_l^{\pm}$ and the φ_l values to the appropriate geometrical features of interfaces are not easy tasks. Indeed, since the pioneering results by Debye & Bueche (1949), Wilson (1949) and Porod (1951), the understanding of these issues has continuously progressed as is testified by the number of papers published over the past decades. [For a recent review see Ciccariello (1993a).]

The present paper illustrates a further relation existing between the $\gamma^{(n)}(0^+)$ values and the geometrical shape of the interface. More definitely, it is shown that: *when the interface consists of planar facets, all the $\gamma^{(n)}(0^+)$'s with $n \geq 4$ are null, $\gamma^{(3)}(0^+)$ is the sum of the contributions owed to each vertex of the interface and each vertex contribution has a closed-form expression dependent only on the angles between the edges entering the vertex.* The first part generalizes the property that all the even derivatives of the CF are null at the origin [i.e. $\gamma^{(2m)}(0^+) = 0$, $m = 1, 2, 3, ...$] when the interfaces are quite smooth (Porod, 1967; Wu & Schmidt, 1971; Ciccariello, 1993c) to interfaces with singularities consisting of linear edges and vertices. The second part is the general solution of the problem (Sobry, Ledent & Fontaine, 1991): to determine the contributions of the singular points of the interface that, added to the Kirste–Porod formula (Kirste & Porod, 1962), yield the exact $\gamma^{(3)}(0^+)$ value. For two-component samples, Kirste & Porod's formula is

$$\mathscr{K}/4V\phi_1\phi_2 \equiv (1/16V\phi_1\phi_2)\int_S dS(3H^2 - \kappa_G)$$

$$= \gamma^{(3)}(0^+), \qquad (1.6)$$

where H and κ_G denote the mean and the Gaussian curvature of the interface. The smoothness of the

interfaces is a necessary condition for the left-hand side (l.h.s.) of (1.6) to be equal to the right-hand side (r.h.s.). Sobry *et al.* (1991) remarked that for right prisms the correct $\gamma^{(3)}(0^+)$ value (Méring & Tchoubar, 1968) is simply obtained by assigning to each vertex a contribution that was explicitly determined (see also Sobry, Fontaine & Ledent, 1994) for vertices with three entering edges and such that two of the three angles formed by the entering edges are equal to $\pi/2$. In this way, Sobry, Fontaine & Ledent essentially conjectured that the exact $\gamma^{(3)}(0^+)$ value can be obtained by adding to the Kirste–Porod value the contributions arising from the singularities of the interfaces. Although the expressions of the contributions due to a general curvilinear edge and to a general contact point are still unknown, the analyses recently undertaken (Ciccariello, 1993a,b; Diez & Sobry, 1993) strongly support this conjecture.* Thus, provided the Kirst-Porod integral exists and is finite,

$$4V\phi_1\phi_2\gamma^{(3)}(0^+) \equiv \mathscr{R} = \mathscr{K} + \mathscr{S}, \qquad (1.7)$$

where $\mathscr{S}$ is related to the singularities of the interface. The quantity on the l.h.s. as well as $\mathscr{K}$ and $\mathscr{S}$ is dimensionless and therefore invariant under scale transformations.

Moreover, $\mathscr{R}$ is proportional to the angular average of the 'rotundity' parameter (Wilson, 1969) and is termed *roundness*. Similarly, $\mathscr{K}$, related to the principal curvatures of the interface, is termed *curvosity*. Finally, $\mathscr{S}$, related both to vertices and to the (curvilinear) edges of the interface, is termed *sharpness*. In this way, (1.7) is equivalent to the statement that *the roundness of a surface is the sum of its curvosity and its sharpness.*

When interfaces have a very arbitrary shape or are related to a very polydisperse sample, it appears reasonable to assume that the sum of the oscillatory contributions, present on the r.h.s. of (1.5), averages to zero owing to their large number.† In these cases, the above statement implies that the intensities scattered by samples whose interfaces consist of planar

---

* It is also noted that, if one assumes that r is in the range $[-\infty, +\infty]$ and then one sets $\gamma(r) \equiv 0$ in the range $r < 0$, the value $r = 0$ becomes a point where the extended $\gamma(r)$ is discontinuous. Thus, the origin can be handled as one of the δ_l's just defined.

---

* It should also be noted that the results obtained by Ciccariello, Cocco, Benedetti & Enzo (1981) and by Ciccariello & Benedetti (1982) for the $\gamma^{(2)}(0^+)$ value indicate that the smooth-interface value $\gamma^{(2)}(0^+) = 0$ must be corrected for possible singularities of the interface and that the correct value is simply obtained by summing up the 'corrections' owed to the interface singularities. Moreover, the non-null contributions to $\gamma^{(2)}(0^+)$ come from edges and contact points only.

† It must be stressed that caution is required in accepting this approximation. In fact, the analysis of the deviations (from a constant behaviour), observed in the Porod plots of the intensities scattered by some demixing glass samples as well as by some coated porous silica samples, yielded quite interesting and consistent information on the microscopic texture of the samples (Benedetti, Ciccariello & Fagherazzi, 1988; Benedetti & Ciccariello, 1994).

facets, asymptotically, are always given by

$$i(h) \equiv I(h)/4\pi V\langle\eta^2\rangle$$

$$\simeq -[2\gamma'(0^+)/h^4] + [4\gamma^{(3)}(0^+)/h^6]. \quad (1.8)$$

The first contribution on the r.h.s. side is the well known Porod term (Porod, 1951; Debye, Anderson & Brumberger, 1957), while the second contribution, owing to the fact that the *curvosity* of planar interfaces is null [see (1.6)], is determined by the interface *sharpness*.

The paper is organized as follows: §II shows that $\gamma(r)$ is a third-degree r polynomial, provided r is sufficiently small; §III shows that $\gamma^{(3)}(0^+)$ is the sum of the contributions owed to each vertex of the interface and reports the closed-form expression of these contributions; §IV illustrates the application of the result to the case of the regular polyhedra. Most of the details on the mathematical manipulations are contained in Appendices *A* and *B*.*

II. General asymptotic expression

The main assumption is (i) that the sample interface consists of planar facets; for simplicity, the analysis is carried out with the further assumption that (ii) the sample comprises only two phases. In §IV, it is briefly discussed how to remove the second assumption and how to make the first weaker. Assumption (ii), (1.2) and (1.4) imply that

$$\gamma''(r) = 1 - P''_{12}(r)/\phi_1\phi_2, \quad (2.1)$$

while (i) implies that the interface singularities are only vertices and edges. First, it must be shown that these singularities do not prevent $\gamma'''(0^+)$ existing. With this aim, owing to (2.1), it is sufficient to prove that, at small r's, $P''_{12}(r)$ can be expanded through the term linear in r. The following analysis will show that, close to the origin, $P''_{12}(r)$ is a linear function of r. This result implies that all the $\gamma^{(n)}(r)$'s, with $n \geq 4$, are equal to zero, so that the first part of the statement is proved. Moreover, if it is assumed that oscillatory contributions can be neglected, (1.8) becomes exact. Otherwise the appropriate oscillatory contributions must be added to (1.8). Finally, the sought-for $\gamma'''(0^+)$ value comes immediately from (2.1) once the coefficient in front of r has been determined in the $P''_{12}(r)$ expression.

The required small-r expansion of $\gamma(r)$ can be obtained starting from the $P''_{12}(r)$ integral expression obtained by Ciccariello *et al.* (1981), namely

$$P''_{12}(r) = -(4\pi V)^{-1} \int \mathrm{d}\,\hat{\omega}\,\mathscr{P}^{(2)}(\hat{\omega},r), \quad (2.2a)$$

where

$$\mathscr{P}^{(2)}(\hat{\omega},r) \equiv \int_{S_1}\mathrm{d}S_1 \int_{S_2}\mathrm{d}S_2(\hat{\sigma}_1 \cdot \hat{\omega})(\hat{\sigma}_2 \cdot \hat{\omega})$$

$$\times \delta(\mathbf{r}_1 + r\hat{\omega} - \mathbf{r}_2). \quad (2.2b)$$

Integral (2.2*a*) expresses $P''_{12}(r)$ as the average, performed over all the possible directions of $\hat{\omega}$, of the quantity $\mathscr{P}^{(2)}(\hat{\omega},r)$ defined by integral (2.2*b*). This integral is performed over S_1 and S_2, *i.e.* the boundaries of phases 1 and 2, while $\hat{\sigma}_1$ is the unit vector pointing outward to phase 1 and orthogonal to S_1 at point $\mathbf{r}_1$ where $\mathrm{d}S_1$ is located. $\hat{\sigma}_2$ and $\mathbf{r}_2$ are similarly defined. It is also noted that assumption (ii) implies that $S_1 = S_2$ and that $\hat{\sigma}_1 = -\hat{\sigma}_2$ at each point of the interface. Finally, $\delta(\mathbf{r})$ denotes Dirac's function. In (2.2*b*), this function requires that $\mathrm{d}S_2$ and $\mathrm{d}S_1$ are at a relative distance r along the direction $\hat{\omega}$. Because the interface consists of planar facets, $S_1 = \cup_l \bar{S}_l$ where $\bar{S}_l$ denotes the *l*th facet of the sample interface. According to (2.2*b*), $\mathscr{P}^{(2)}(\hat{\omega},r)$ is equal to the sum of the values obtained from (2.2*b*) by identifying S_1 and S_2 with all possible pairs of facets. Thus,

$$\mathscr{P}^{(2)}(\hat{\omega},r) = \sum_{i,l} \mathscr{P}^{(2)}_{i,l}(\hat{\omega},r), \quad (2.3)$$

where

$$\mathscr{P}^{(2)}_{i,l}(\hat{\omega},r) \equiv \int_{\bar{S}_i}\mathrm{d}S_1 \int_{\bar{S}_l}\mathrm{d}S_2(\hat{\sigma}_i \cdot \hat{\omega})(\hat{\sigma}_l \cdot \hat{\omega})$$

$$\times \delta(\mathbf{r}_1 + r\hat{\omega} - \mathbf{r}_2). \quad (2.4)$$

However: (*a*) when the facet pair involves the same facet, integral (2.4) is null because $\hat{\omega}$, lying in the facets' plane, is orthogonal to $\hat{\sigma}_i$ as well as to $\hat{\sigma}_l$; (*b*) when the pair involves two facets that have no point in common, the facets will be separated by a finite distance, say D, and when $r < D$, no $\bar{S}_i$ subset is r apart from $\bar{S}_l$ and integral (2.4) vanishes owing to the presence of Dirac's function; (*c*) therefore, at sufficiently small r's, only the pairs of facets, which have in common either one edge or one vertex, can make $P''_{12}(r) \neq 0$. The second of these configurations can be obtained by considering a configuration of the first kind (*i.e.* two facets meeting along a 'finite' edge, where 'finite' means that the length of the edge is different from zero), and then by letting the edge shrink to a point. For this reason, the case depicted in Fig. 1, where the two facets ($\bar{S}_1$ and $\bar{S}_2$) share the finite edge VV', is analysed first. In order to evaluate the relevant $\mathscr{P}^{(2)}_{1,2}(\hat{\omega},r)$ contribution, it is convenient to introduce two Cartesian coordinate systems: $Vxyz$ and $VXYZ$ (see Fig. 1). Axes z and Z coincide with the common edge VV'. Coinciding axes x and X are orthogonal to VV' and lie on the $\bar{S}_1$ half-plane. System $Vxyz$ is orthogonal, while system $VXYZ$ is only Cartesian because axis Y, orthogonal to $z = Z$, lies in the half-plane containing facet $\bar{S}_2$. For each vertex, say V, the relevant edges will be oriented as

coming out from V and will be denoted l_1, l_2 and l_3, depending on whether they lie on $\overline{S}_1$, $\overline{S}_2$ or the common edge. Moreover, the angles that l_1 and l_2 form with the third (common) edge $l_3 = z = Z$ and the angle that l_1 makes with l_2 will be respectively denoted γ_2, γ_1 and γ_3. The dihedral angles formed by the pairs of planes $[(l_1,l_3), (l_2,l_3)]$, $[(l_1,l_2), (l_3,l_2)]$ and $[(l_3,l_1), (l_2,l_1)]$ are denoted α_3, α_2 and α_1. With these angles so defined, the constraints

$$0 \le \gamma_i \le \pi, \quad 0 \le \alpha_i \le \pi, \quad i = 1, 2, 3 \qquad (2.5)$$

are applicable. Later, it will be useful to look at the γ_i's as the sides of a spherical triangle and at the α_i's as the corresponding angles (see Fig. 2). It is also noted that the dihedral angles α_i are related to the edge angles γ_i by the relation [see (4.3.19) of Abramowitz & Stegun, 1972]

$$\cos \gamma_l = \cos \gamma_i \cos \gamma_j + \sin \gamma_i \sin \gamma_j \cos \alpha_l, \qquad (2.6)$$

where i, j, l is any cyclic permutation of 1, 2, 3. It is also convenient to set

$$c_i \equiv \cot \gamma_i, \quad i = 1, 2, 3. \qquad (2.7)$$

Quantities c_i', l_i', γ_i' and α_i' ($i = 1, 2, 3$) are similarly defined (see Fig. 1). In particular, it should be noted that l_3' and l_3 have opposite directions. By parameterization of the points of $\overline{S}_1$ and $\overline{S}_2$ in terms of the $VXYZ$ coordinate system, the integration domains,
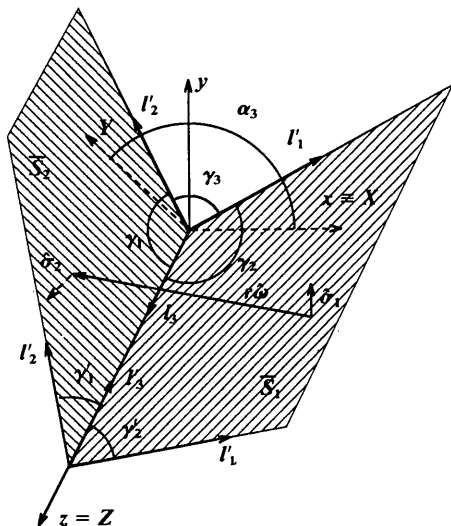

Fig. 1. Typical configuration of two planar facets, $\overline{S}_1$ and $\overline{S}_2$, meeting along a non-null edge (VV'). l_1, l_3 and l_1' are the sides of $\overline{S}_1$ nearest to the edge. In the definition of the angles γ_1, γ_2 and γ_3, the edges l_1, l_2 and $l_3 = VV'$, meeting at V, are oriented away from V. Axes x and X coincide. They lie on the $\overline{S}_1$ half-plane and are orthogonal to $z = Z = l_3$. Axis y is orthogonal to x and z, while axis Y is orthogonal to z and lies on the $\overline{S}_2$ half-plane. Phase 1 (2) fills in the region below (above) $\overline{S}_1$ and on the left (right) of $\overline{S}_2$. Thus, at point P_1, the unit vector $\hat{\sigma}_1$ is parallel to y, while at point P_2, as shown, $\hat{\sigma}_2$ points towards the bottom left of $\overline{S}_2$.

related to the presence of edges l_i and l_i', can easily be handled on the r.h.s. of (2.4). In this way, the explicit evaluation of $\mathscr{P}_{\overline{1},\overline{2}}^{(2)}(\hat{\omega},r)$, the contribution to $\mathscr{P}^{(2)}(\hat{\omega},r)$ arising from facet pair $(\overline{1},\overline{2})$, becomes quite easy. (Note that the overbar over a numerical index value indicates the facet labelled by that value.) With reference to Appendix A for the detailed reduction of (1.4), the final result is either

$$\mathscr{P}_{\overline{1},\overline{2}}^{(2)}(\hat{\omega},r) = e_{\overline{1},\overline{2}}(\hat{\omega})[L_{\overline{1},\overline{2}} - r(\mathscr{W} + \mathscr{W}')] \qquad (2.8a)$$

or

$$\mathscr{P}_{\overline{1},\overline{2}}^{(2)}(\hat{\omega},r) = -r e_{\overline{1},\overline{2}}(\hat{\omega})(\mathscr{W} + \mathscr{W}')\Theta(-\mathscr{W} - \mathscr{W}'), \qquad (2.8b)$$

depending on whether $L_{\overline{1},\overline{2}}$, the length of the edge between facets $\overline{S}_1$ and $\overline{S}_2$, is different or equal to zero, respectively. The remaining quantities* $\mathscr{W}$, $\mathscr{W}'$ and $e_{\overline{1},\overline{2}}$ are defined as follows:

$$\mathscr{W} = \mathscr{W}(\gamma_1, \gamma_2, \alpha_3; \hat{\omega})$$
$$\equiv \max[(c_2\omega_y/\sin \alpha_3) - \omega_z, \ c_1(\omega_y \cot \alpha_3 - \omega_x)], \qquad (2.9a)$$

$$\mathscr{W}' = \mathscr{W}'(\gamma_1', \gamma_2', \alpha_3; \hat{\omega})$$
$$\equiv \mathscr{W}(\gamma_1', \gamma_2', \alpha_3; \omega_x, \omega_y, -\omega_z), \qquad (2.9b)$$

$$e_{\overline{1},\overline{2}}(\hat{\omega}) \equiv (\hat{\sigma}_{\overline{1}} \cdot \hat{\omega})(\hat{\sigma}_{\overline{2}} \cdot \hat{\omega})\Theta(\hat{\sigma}_{\overline{1}} \cdot \hat{\omega})\Theta(\hat{\sigma}_{\overline{2}} \cdot \hat{\omega})/\sin \alpha_3. \qquad (2.10)$$

Here, $\Theta(x)$ denotes the Heaviside step function defined as being equal to one on the positive axis and zero elsewhere.

The first consequence of (2.8a) and (2.8b) is that $\mathscr{P}_{\overline{1},\overline{2}}^{(2)}(\hat{\omega},r)$, whatever the length of the edge, is exactly linear with respect to r, when r is sufficiently small.

---

* In order to avoid cumbersome notation, $\mathscr{W}$ and $\mathscr{W}'$ do not have the indices characterizing the facet pair. Strictly speaking, for each pair of facets, the introduction of $\mathscr{W}$ and $\mathscr{W}'$ implies that the considered facets are identified with those of Fig. 1. In this way, a suitable relabelling of angles has to be undertaken.
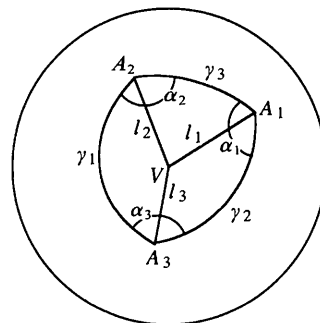

Fig. 2. $A_1A_2A_3$ is the spherical triangle associated with edges l_1, l_2 and l_3 shown in Fig. 1. Its sides γ_1, γ_2 and γ_3 are the angles between the edges l_2 and l_3, l_1 and l_3, l_1 and l_2. Its angles α_i, $i = 1, 2, 3$, are the dihedral angles formed by the plane (l_1,l_2) with (l_1,l_3), by (l_2,l_1) with (l_2,l_3), and by (l_3,l_1) with (l_3,l_2), respectively.

[The precise meaning of this locution will be evident from the $\mathscr{P}_{1,2}^{(2)}(\hat{\omega},r)$ evaluation reported in Appendix A.] Since $\mathscr{P}^{(2)}(\hat{\omega},r)$ is a sum of contributions $\mathscr{P}_{i,l}^{(2)}(\hat{\omega},r)$ [see (2.3)], the linearity property also holds true for $\mathscr{P}^{(2)}(\hat{\omega},r)$ and, by (2.2a) and (2.1), for $P_{12}^{(2)}(r)$ and $\gamma^{(2)}(r)$. It is concluded that

$$\gamma^{(n)}(0^+) = 0, \quad n = 4, 5, 6, ..., \qquad (2.11)$$

when interfaces are made up of planar facets. This proves the statement that the asymptotic expansion of $I(h)$ contains the only two monotonically decreasing terms reported on the r.h.s. of (1.8).* Equations (2.8a,b), evaluated at $r = 0^+$, give

$$\mathscr{P}_{i,l}^{(2)}(\hat{\omega},0^+) = e_{i,l}(\hat{\omega})L_{i,l}, \qquad (2.12)$$

while (2.3), (2.10), (2.2a) and (2.1) yield

$$\gamma''(0^+) = (1/4\pi V\phi_1\phi_2) \sum_{i,l} L_{i,l} \int e_{i,l}(\hat{\omega})d\hat{\omega}. \qquad (2.13)$$

The integral is easily evaluated and the result, first obtained by Ciccariello *et al.* (1981), shows that $\gamma^{(2)}(0^+)$ is the sum of the contributions arising from each edge of the sample interface. Moreover, result (2.13) also holds true when edges are curvilinear and surfaces are no longer planar.

III. General vertex contribution

Two further consequences can be drawn from (2.8a) and (2.8b), namely: (α) $\gamma^{(3)}(0^+)$ can be expressed as a sum of contributions each orginating from a vertex of the interface and (β) each of these contributions can be explicitly written down in terms of the angles between the edges entering the considered vertex.

Thus, one must evaluate the r derivatives of contributions (2.8a) and (2.8b), remembering that these are related to facet pair $(\bar{1},\bar{2})$ when the facets meet along a finite or a null-length edge, respectively. As $r \to 0^+$, is is found that

$$\mathscr{P}_{1,2}^{(3)}(\hat{\omega},0^+) = d\mathscr{P}_{1,2}^{(2)}(\hat{\omega},r)/dr|_{r=0^+}$$

$$= [\mathscr{S}_{3;(\bar{1},\bar{2})}(\hat{\omega}) + \mathscr{S}'_{3;(\bar{1},\bar{2})}(\hat{\omega})] \qquad (3.1)$$

or

$$\mathscr{P}_{1,2}^{(3)}(\hat{\omega},0^+) = \mathscr{S}_{4;(\bar{1},\bar{2})}(\hat{\omega}), \qquad (3.2)$$

where

$$\mathscr{S}_{3;(\bar{1},\bar{2})}(\hat{\omega}) \equiv -e_{\bar{1},\bar{2}}(\hat{\omega})\mathscr{W}, \qquad (3.3a)$$

$$\mathscr{S}'_{3;(\bar{1},\bar{2})}(\hat{\omega}) \equiv -e_{\bar{1},\bar{2}}(\hat{\omega})\mathscr{W}', \qquad (3.3b)$$

$$\mathscr{S}_{4;(\bar{1},\bar{2})}(\hat{\omega}) \equiv -e_{\bar{1},\bar{2}}(\hat{\omega})(\mathscr{W} + \mathscr{W}')$$

$$\times \Theta(-\mathscr{W} - \mathscr{W}'). \qquad (3.4)$$

[Although the argument 0^+ present in the functions on the l.h.s. of (3.1) and (3.2) is superfluous, because the r derivative of $\mathscr{P}_{1,2}^{(2)}(\hat{\omega},r)$ is independent of r when r is close to the origin, its introduction is a useful reminder of this condition and makes the calculation of $\gamma'''(0^+)$ easier.]

Clearly, when the edge length is null, the facets can meet only at a vertex, say V, of the interface. Then (3.2) can be considered as one of the contributions related to V, since it arises from one of the pairs of facets [*i.e.* $(\bar{S}_1,\bar{S}_2)$] that meet at V. Besides, definitions (2.9a), (2.9b) and (2.10) show that $\mathscr{S}_{1;(\bar{1},\bar{2})}$ depends only on angles that are simply related to $\bar{S}_1$'s edges: l_1 and l'_1 and to $\bar{S}_2$'s edges: l_2 and l'_2. Thus, $\mathscr{S}_{4;(\bar{1},\bar{2})}$ is the contribution arising from vertex V and from the *four* edges l_1, l'_1, l_2 and l'_2. For this reason, $\mathscr{S}_{4;(i,l)}$, as it is specified by its first index value 4, will be generally referred to as a *four-edge* (vertex) contribution. Consider now the case of two facets meeting along a finite edge, say VV'. This determines two vertices of the interface, say V and V', and (3.1) shows that the contribution owed to the considered facet pairs is the sum of the two terms $\mathscr{S}_{3;(\bar{1},\bar{2})}$ and $\mathscr{S}'_{3;(\bar{1},\bar{2})}$. From (3.3), (2.9$a$) and (2.10), it appears evident that $\mathscr{S}_{3;(\bar{1},\bar{2})}$ and $\mathscr{S}'_{3;(\bar{1},\bar{2})}$ depend, respectively, only on the angles formed by the three edges (l_1, l_2, l_3) entering vertex V and on the angles formed by the edges (l'_1, l'_2, l'_3) entering vertex V'. It is concluded that contribution (3.1), related to a pair of facets meeting along a finite edge, can be expressed as a sum of *three-edge* (vertex) contributions.

Consider now the general case. The derivative of (2.3), at $r = 0^+$, is

$$\mathscr{P}^{(3)}(\hat{\omega},0^+) = \sum_{i,l}' \mathscr{P}_{i,l}^{(3)}(\hat{\omega},0^+). \qquad (3.5)$$

The prime is a reminder that the summation is restricted to the pairs of facets that have at least one point in common. Considered now a vertex V of the interface and consider all the different pairs of facets meeting at V. For each of these pairs, either the facets meet only at V or the facets have an edge in common. In the first case, the contribution that has to be considered on the r.h.s. of (3.5) is given by (3.4), in the second case, it is given by (3.3a) or (3.3b). Clearly, the sum present on the r.h.s. of (3.5) is recovered by summing the vertex contributions of all the facet pairs relevant to a vertex and then over all the vertices. In this way, $\mathscr{P}^{(3)}(\hat{\omega},0^+)$ is expressed as a sum of vertex contributions. Owing to (2.2a)

---

* This result is of some relevance to wide-angle X-ray scattering. It implies that, aside from oscillatory deviations, the decrease of the peak profiles, in the ideal cases where sample particles can be depicted as homogeneous regions with planar boundaries, is given by the sum $A/h^2 + B/h^4$ with A and B related, respectively, to the projected surface and to the 'rotundity' of the crystallites (Wilson, 1949, 1969, 1970; Ciccariello, 1990, 1993a).

and (2.1), the same property holds true for $\gamma^{(3)}(0^+)$:

$$\gamma^{(3)}(0^+) = \sum_{V_l}(2/4\pi V\phi_1\phi_2)\int\left[\sum_{i<j}{}'\mathscr{E}_{3;(i,j)}(\hat{\omega})\right.$$

$$\left. + \sum_{i<j}{}'\mathscr{E}_{4;(i,j)}(\hat{\omega})\right]d\hat{\omega}. \qquad (3.6)$$

The primes now indicate that the sums are restricted to the only pairs of facets that meet at a given vertex, i.e. V_l. Moreover, the internal sums involve only the pairs that consist of different facets because the factor 2 already accounts for the two possible ways of ordering two facets in forming a pair. Finally, no $\mathscr{E}'_{3;(i,j)}$ appears in (3.6) because the simple change of integration variable $\hat{\omega} = (\hat{\omega}_x,\hat{\omega}_y,\hat{\omega}_z)\to(\hat{\omega}_x,\hat{\omega}_y,-\hat{\omega}_z) = \hat{\omega}'$ converts the previous function in $\mathscr{E}_{3;(i,j)}$. This is evident by comparing (2.9b) and (2.9a) and noting that $e_{i,j}(\hat{\omega})$ is independent of $\hat{\omega}_z$, $\hat{\sigma}_i$ and $\hat{\sigma}_j$ being orthogonal to z. If we now set

$$\mathscr{V}_{3;(i,j)} = 2\int\mathscr{E}_{3;(i,j)}(\hat{\omega})d\hat{\omega} \qquad (3.7a)$$

$$\mathscr{V}_{4;(i,j)} = 2\int\mathscr{E}_{4;(i,j)}(\hat{\omega})d\hat{\omega}, \qquad (3.7b)$$

(3.6) becomes

$$\gamma^{(3)}(0^+) = (1/4\pi V\phi_1\phi_2)\sum_{V_l}\left[\sum_{i<j}{}'\mathscr{V}_{3;(i,j)} + \sum_{i<j}{}'\mathscr{V}_{4;(i,j)}\right]. \qquad (3.8)$$

Since all the contributions inside the square brackets refer to vertex V_l, their sum represents the total contribution of vertex V_l and property (α), stated at the beginning of the section, is proven.

In order to prove property (β), it will be sufficient to show that each contribution present on the r.h.s. of (3.8) can be evaluated in closed form. This is done in two steps. First, it is shown that each four-edge vertex contribution is a linear combination of four three-edge vertex contributions. Second, the closed expression of a three-edge vertex contribution is obtained.

Fig. 3 shows a typical four-edge vertex where, for notational simplicity, the meeting facets are again characterized by indices $\bar{1}$ and $\bar{2}$. Facets $\bar{S}_1$ and $\bar{S}_2$ are prolonged until they meet along a half-line, called $\bar{I}_{\bar{1},\bar{2}}$. The prolonged facets are denoted $\bar{S}_{\bar{1}p}$ and $\bar{S}_{2p}$, while the facets added to the outset facets in order to have the prolonged ones, are respectively denoted $\bar{S}_{1a}$ and $\bar{S}_{1a}$. Now, according to definition (2.4), imagine evaluating

$$\mathscr{P}^{(2)}_{\bar{1}p,\bar{2}p}(\hat{\omega},r) \equiv \int\limits_{\bar{S}_{1p}} dS_1 \int\limits_{\bar{S}_{2p}} dS_2(\hat{\sigma}_{\bar{1}}\cdot\hat{\omega})(\hat{\sigma}_{\bar{2}}\cdot\hat{\omega})$$

$$\times \delta(\mathbf{r}_1 + r\hat{\omega} - \mathbf{r}_2), \qquad (3.9a)$$

at very small r's, so that only small regions around vertex V will contribute to the integral. Since $\bar{S}_{ip} =$

$\bar{S}_i\cup\bar{S}_{ia}$ with $i = \bar{1}, \bar{2}$,

$$\mathscr{P}^{(2)}_{\bar{1}p,\bar{2}p}(\hat{\omega},r) = \mathscr{P}^{(2)}_{\bar{1},\bar{2}}(\hat{\omega},r) + \mathscr{P}^{(2)}_{\bar{1}a,\bar{2}}(\hat{\omega},r)$$

$$+ \mathscr{P}^{(2)}_{\bar{1},\bar{2}a}(\hat{\omega},r) + \mathscr{P}^{(2)}_{\bar{1}a,\bar{2}a}(\hat{\omega},r). \qquad (3.9b)$$

By adding and subtracting $\mathscr{P}^{(2)}_{\bar{1}a,\bar{2}a}(\hat{\omega},r)$ and observing that

$$\mathscr{P}^{(2)}_{\bar{1}a,\bar{2}p}(\hat{\omega},r) = \mathscr{P}^{(2)}_{\bar{1}a,\bar{2}}(\hat{\omega},r) + \mathscr{P}^{(2)}_{\bar{1}a,\bar{2}a}(\hat{\omega},r),$$

$$\mathscr{P}^{(2)}_{\bar{1}p,\bar{2}a}(\hat{\omega},r) = \mathscr{P}^{(2)}_{\bar{1},\bar{2}a}(\hat{\omega},r) + \mathscr{P}^{(2)}_{\bar{1}a,\bar{2}a}(\hat{\omega},r),$$

from (3.9b), one obtains the result

$$\mathscr{P}^{(2)}_{\bar{1},\bar{2}}(\hat{\omega},r) = \mathscr{P}^{(2)}_{\bar{1}p,\bar{2}p}(\hat{\omega},r) + \mathscr{P}^{(2)}_{\bar{1}a,\bar{2}a}(\hat{\omega},r)$$

$$- \mathscr{P}^{(2)}_{\bar{1}p,\bar{2}a}(\hat{\omega},r) - \mathscr{P}^{(2)}_{\bar{1}a,\bar{2}p}(\hat{\omega},r). \qquad (3.10)$$

The importance of this result stems from the fact that all quantities present on the r.h.s. refer to configurations where the meeting surfaces share an edge (i.e. $\bar{I}_{\bar{1},\bar{2}}$). Hence, by taking the derivative of (3.10) with respect to r and integrating with respect to $\hat{\omega}$, one obtains the required result

$$\mathscr{V}_{4,(\bar{1},\bar{2})} = \mathscr{V}_{3,(\bar{1}p,\bar{2}p)} + \mathscr{V}_{3,(\bar{1}a,\bar{2}a)} - \mathscr{V}_{3,(\bar{1}p,\bar{2}a)} - \mathscr{V}_{3,(\bar{1}a,\bar{2}p)},$$

$$(3.11)$$

expressing a four-edge vertex contribution in terms of four three-edge vertex contributions. The edge triplets and the signs, correspondingly associated with the four-edge contribution, are (see Fig. 3)

$$+ (l_1, l_2, \bar{I}_{\bar{1},\bar{2}}), \quad + (l'_1, l'_2, \bar{I}_{\bar{1},\bar{2}}), \quad - (l'_1, l_2, \bar{I}_{\bar{1},\bar{2}})$$

$$\text{and} \quad - (l_1, l'_2, \bar{I}_{\bar{1},\bar{2}}). \qquad (3.12)$$
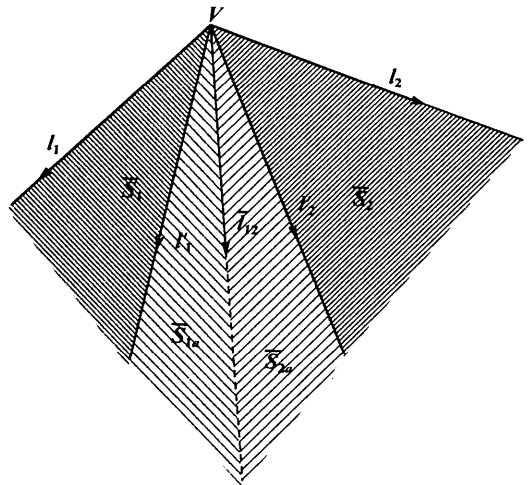

Fig. 3. The figure shows two facets ($\bar{S}_1$ and $\bar{S}_2$), which meet only at vertex V. When the facets are prolonged, they will intersect along the 'edge' $\bar{I}_{\bar{1},\bar{2}}$. $\bar{S}_{1a}$ shows the planar surface, which, added to $\bar{S}_1$, gives the prolonged facet $\bar{S}_{1p}$. $\bar{S}_{2a}$ and $\bar{S}_{2p}$ are similarly defined.

The last task is that of obtaining the closed-form expression of $\mathscr{V}_{3;(i,j)}$. By the same convention expounded in the footnote * on p. 63 and by (3.3), the typical $\mathscr{V}_{3;(i,j)}$ can be written as

$$\mathscr{V}(\gamma_1, \gamma_2, \alpha_3) \equiv \mathscr{V}_{3;(\bar{1},\bar{2})}$$
$$= -2\int d\hat{\omega} e_{\bar{1},\bar{2}}(\hat{\omega}) \mathscr{W}(\gamma_1, \gamma_2, \alpha_3; \hat{\omega}),$$
$$(3.13)$$

where α_3 is the dihedral angle between the meeting facets and γ_1 and γ_2 are the angles formed by edges l_2 and l_1 with edge l_3, intersection of the two (prolonged) facets. The reduction of this integral is rather involved. Therefore, its explicit evaluation is given in Appendix B.† The final result is

$$\mathscr{V}(\gamma_1, \gamma_2, \alpha_3)$$
$$= -\tfrac{1}{4}\{1 - (\pi - \gamma_3)$$
$$\times [c_3 - (2\cot\alpha_3 \sin\gamma_3/\sin\alpha_3 \sin\gamma_1 \sin\gamma_2)]$$
$$+ 2[c_1\gamma_2 + c_2\gamma_1](\cot\alpha_3/\sin\alpha_3)$$
$$+ [c_1(\pi - \gamma_1) + c_2(\pi - \gamma_2)](1 + 2\cot^2\alpha_3)\}.$$
$$(3.14)$$

An equivalent form is

$$\mathscr{V}(\gamma_1, \gamma_2, \alpha_3)$$
$$= -\tfrac{1}{4}\{1 + 2\pi[\cot\alpha_3(\cot\gamma_1 + \cot\gamma_2)/\sin\alpha_3]$$
$$+ (\pi - \gamma_1)[\cot\gamma_1 - 2(\cot\alpha_3 \cot\alpha_2/\sin\gamma_1)]$$
$$+ (\pi - \gamma_2)[\cot\gamma_2 - 2(\cot\alpha_3 \cot\alpha_1/\sin\gamma_2)]$$
$$- (\pi - \gamma_3)[\cot\gamma_3$$
$$- 2(\cot\alpha_3 \sin\gamma_3/\sin\gamma_1 \sin\gamma_2 \sin\alpha_3)]\}. \quad (3.15)$$

These results are respectively obtained by combing equation (B.40) or equation (B.41) with equation (B.6). Since the dihedral angles α_i are related to the edge angles γ_i by relation (2.6), either the γ_i's or the α_i's could be used in (3.14) and (3.15). Besides, $\mathscr{V}(\gamma_1, \gamma_2, \alpha_3)$ turns out to be either positive or negative depending on the γ_i values. The result obtained by Sobry et al. (1991) is immediately recovered when two of the three γ_i's [recall (2.6)] are equal to $\pi/2$.

IV. Concluding remarks

It has been shown that, in the case of two-component samples, planar interfaces yield CFs that, close to the origin, are third-degree polynomials in r. Hence, there is the interesting result that the relevant SAS intensities, asymmptotically, present only two monotonically decreasing terms. The first is the Porod contribution; the second is the Kirste–Porod

† See deposition footnote.

Table 1. Roundness of regular polyhedra

	$\mathscr{N}_v$	$\mathscr{N}_e$	$\mathscr{N}_4$	$\mathscr{R} = \mathscr{S}$	$4V_p\mathscr{N}_e\mathscr{V}_{3,(i,j)}$	$4V_p\mathscr{N}_4\mathscr{V}_{4,(i,j)}$
Tetrahedron	4	3	0	−5.285	−1.321	0.000
Cube	8	3	0	−1.910	−0.239	0.000
Dodecahedron	20	3	0	−0.361	−0.018	0.000
Octahedron	6	4	2	0.626	−0.492	0.596
Icosahedron	12	5	5	2.337	−0.188	0.383

The table reports the *sharpness*, coinciding with the *roundness*, of the regular polyhedra. [Recall that, when the sample comprises a single particle, definition (1.7) becomes $\mathscr{R} = 4V_p\gamma^{(3)}(0^+)$, because the quantity $V\phi_1\phi_2$ must be substituted for V_p, the particle volume.] Moreover, $\mathscr{N}_v$ is the number of the particle vertices, $\mathscr{N}_e$ that of the edges entering a particle vertex or that of the three-edge contributions at a vertex and $\mathscr{N}_4$ is the number of the four-edge contributions per vertex. Finally, $4V_p\mathscr{N}_e\mathscr{V}_{3,(i,j)}$ and $4V_p\mathscr{N}_4\mathscr{V}_{4,(ij)}$, respectively, are the sums of the three-edge and four-edge contributions to $\mathscr{R}$ owed to a particle vertex. In other words, they are equal to $4V_p$ times the first or the second sum inside the square brackets on the r.h.s of (3.8). It should be noted that $\mathscr{R}$ approches 2π, the sphere value, as the number of the edges entering each vertex increases.

contribution. This is determined by the $\gamma^{(3)}(0^+)$ value. When the sample interface contains vertices with only three entering edges, (3.8) and (3.14) or (3.15) easily allow the determination of $\gamma^{(3)}(0^+)$ in a closed form once the angles, between the edges entering each vertex have been calculated. On the other hand, when the interface presents vertices with four or more entering edges, then, for each of these vertices, the relevant three-edge as well as four-edge contributions must be taken into account. The first are calculated by (3.14). The second are first expressed in terms of three-edge contributions by (3.11) and (3.12) and then explicitly calculated by (3.14) or (3.15). As an application, the $\gamma^{(3)}(0^+)$ values relevant to the regular polyhedra have been evaluated. Their values are reported in Table 1.

The generalization of the previous results to the case of N-component samples is trivial. Appropriate indices for a proper book-keeping of the different phases have to be introduced and due attention must be paid to the fact that the factor $1/(\phi_1\phi_2)$ becomes $(n_i - n_j)^2/\langle\eta^2\rangle$.

Similarly to the discussion reported after (2.13), results (3.8) and (3.7) also hold true when the interface no longer consists of planar facets and presents vertices with entering edges that result from the intersection of curved facets. In proximity to each vertex, say V, each curved facet can be approximated by its tangent planar angle, defined as the intersection of the plane, tangent to the curved facet at V, with the lines tangent at V to the two edges delimiting the curved facet. From this point of view, (3.8) represents the 'correction' arising from a vertex to the Kirste–Porod formula. Beside this correction, those related to the edges, when these are curvilinear, and to the contact points, present only on curved

interfaces, should be added. So far, the edge corrections have been worked out only for some particularly simple geometries (Ciccariello, 1993a,b; Diez & Sobry, 1993). Therefore, the problem of determining the 'roundness' of an interface, i.e. its $\gamma^{(3)}(0^+)$ value, in the presence of vertices, curvilinear edges and contact points, requires the determination of the 'corrections' associated with general curved edges and contact points to be completely solved. With curved interfaces, however, further monotonically decreasing terms will be present on the r.h.s. of (1.8). They are related to the $\gamma^{(2n+1)}(0^+)$ values with $n \geq 2$. Similarly to the $\gamma^{(3)}(0^+)$ expression, (1.6), the higher-order derivatives can also be expressed as interface averages of appropriate combinations of the derivatives of the parametric equations of the sample interface, provided the interface is sufficiently smooth. Indeed, the explicit expressions of $\gamma^{(5)}(0^+)$ and $\gamma^{(7)}(0^+)$ have been reported by Wu & Schmidt (1971) and Ciccariello (1993c). At this point, similarly to the $\gamma^{(2)}(0^+)$ and $\gamma^{(3)}(0^+)$ cases, there is the problem of evaluating the 'corrections' associated with edges, vertices and contact points for the higher-order derivative values $\gamma^{(n)}(0^+)$, $n = 4, 5, \ldots$. Of course, the problem appears to be far more difficult than that analysed here. From a practical point of view, however, it looks less interesting, owing to the great simplicity and generality of the interface analysed in this paper.

APPENDIX A

From Fig. 1, it appears evident that the (X, Y, Z) and (x, y, z) coordinates are related as follows

$$X = x - y \cot \alpha_3, \qquad (A.1a)$$

$$Y = y/\sin \alpha_3, \qquad (A.1b)$$

$$Z = z. \qquad (A.1c)$$

Moreover, the equations of half-lines l_1 and l_2 are

$$y_1 = 0, \quad z_1 = c_2 x, \quad x \geq 0, \qquad (A.2a)$$

$$X_2 = 0, \quad z_2 = c_1 Y, \quad Y \geq 0, \qquad (A.2b)$$

while those of l_1' and l_2' are

$$y_1' = 0, \quad z_1' = L_{\bar{1},\bar{2}} - c_2' x, \quad x \geq 0, \qquad (A.3a)$$

$$X_2' = 0, \quad z_2' = L_{\bar{1},\bar{2}} - c_1' Y, \quad Y \geq 0, \qquad (A.3b)$$

where c_i and c_i' are defined by (2.7) and $L_{\bar{1},\bar{2}}$ denotes the length of edge VV'. According to (2.4), the contribution from facets $\bar{S}_1$ and $\bar{S}_2$ to $\mathcal{P}^{(2)}(\hat{\omega}, r)$ is

given by

$$\mathcal{P}_{\bar{1},\bar{2}}^{(2)}(\hat{\omega}, r) = (\hat{\sigma}_1 \cdot \hat{\omega})(\hat{\sigma}_2 \cdot \hat{\omega}) \int dx_1 \int_{z_1(x_1)}^{z_1'(x_1)} dz_1 \int dY_2$$

$$\times \int_{z_2(Y_2)}^{z_2'(Y_2)} dz_2 \delta(x_1 + r\omega_x - x_2)$$

$$\times \delta(y_1 + r\omega_y - y_2)\delta(z_1 + r\omega_z - z_2),$$
$$(A.4)$$

where the properties $dS_1 = dx_1 dz_1$ and $dS_2 = dY_2 dz_2$ have been used. The analytical expressions of the integration limits are given by $(A.2)$ and $(A.3)$. The arguments of Dirac's function involve the orthogonal coordinates (x_1, y_1, z_1) and (x_2, y_2, z_2) of two points lying, respectively, on $\bar{S}_1$ and $\bar{S}_2$. The two points are required to be r apart. The quantity r, at the end of the calculations, has to go to zero. Thus, only small strips of $\bar{S}_1$ and $\bar{S}_2$, parallel to edge VV', will contribute to the integral. It is important to note that this condition becomes true once r has become smaller than the smallest of the two distances $H_{\bar{1}}$ and $H_{\bar{2}}$, $H_{\bar{1}}$ ($H_{\bar{2}}$) being the distance of the $\bar{S}_1$ ($\bar{S}_2$) facet vertex, which does not lie on the edge, from the plane of facet $\bar{S}_2$ ($\bar{S}_1$). In this range of r's, the integration-domain upper limits, not specified in $(A.4)$, can be set equal to $+\infty$. It is now noted that the points belonging to $\bar{S}_1$ have $y_1 = 0$ and that the orthogonal coordinates of an $\bar{S}_2$ point, characterized by coordinates $(0, Y_2, Z_2)$ in the system $VXYZ$, are $[-Y_2 \sin(\alpha_3 - \pi/2), Y_2 \cos(\alpha_3 - \pi/2), z_2]$. Thus, the argument $y_1 + r\omega_y - y_2$ of the second δ function on the r.h.s. of $(A.4)$ becomes $y_1 + r\omega_y - Y_2 \sin \alpha_3$. Now, the third Dirac function on the r.h.s. of $(A.4)$ requires that

$$z_2 = z_1 + r\omega_z. \qquad (A.5a)$$

For the corresponding integral to be different from zero, the previous value must be smaller than $z_2'(Y_2)$ and greater than $z_2(Y_2)$. Similarly, the second Dirac function requires $y_2 = r\omega_y$, which by $(A.1a)$ and $(A.1b)$, implies

$$Y_2 \equiv \bar{Y}_2 = r\omega_y/\sin \alpha_3, \qquad (A.5b)$$

$$x_2 = \bar{Y}_2 \cos \alpha_3 = r\omega_y \cot \alpha_3. \qquad (A.5c)$$

By these equations and the integration bound $\bar{Y}_2 \geq 0$, $(A.4)$ becomes

$$\mathcal{P}_{\bar{1},\bar{2}}^{(2)}(\hat{\omega}, r) = [(\hat{\sigma}_1 \cdot \hat{\omega})(\hat{\sigma}_2 \cdot \hat{\omega})\Theta(\bar{Y}_2)/\sin \alpha_3]$$

$$\times \int_0^\infty dx_1 \delta(x_1 + r\omega_x - r\omega_y \cot \alpha_3)$$

$$\times \int_{z_1(x_1)}^{z_1'(x_1)} dz_1 \Theta[z_2'(\bar{Y}_2) - z_1 - r\omega_z]$$

$$\times \Theta[z_1 + r\omega_z - z_2(\bar{Y}_2)]. \qquad (A.6)$$

Owing to the first Θ function, present inside the z_1 integral, and to the presence of an upper integration limit, z_1 must be smaller than $\min\,[z_2'(\overline{Y}_2) - r\omega_z, z_1'(x_1)]$. For similar reasons, z_1 must be larger than $\max\,[z_2(\overline{Y}_2) - r\omega_z, z_1(x_1)]$. Therefore, the integral with respect to z_1 is equal to the difference of the quantities just reported when the difference is positive, otherwise it is null. The remaining integral with respect to x_1 is immediately performed since the remaining δ function requires

$$x_1 = \overline{X}_1 \equiv r(\omega_y \cot \alpha_3 - \omega_x). \qquad (A.7)$$

Of course, this value must be positive. It is concluded that

$$\mathscr{P}_{\overline{1},2}^{(2)}(\hat{\omega},r) = e_{\overline{1},2}\mathscr{D}_{\overline{1},2}\Theta(\mathscr{D}_{\overline{1},2}) \qquad (A.8a)$$

where

$$\mathscr{D}_{\overline{1},2} \equiv \min\,[z_1'(\overline{X}_1),z_2'(\overline{Y}_2) - r\omega_z]$$
$$- \max\,[z_1(\overline{X}_1),z_2(\overline{Y}_2) - r\omega_z], \qquad (A.8b)$$

$$e_{\overline{1},2} \equiv (\hat{\sigma}_1 \cdot \hat{\omega})(\hat{\sigma}_2 \cdot \hat{\omega})\Theta(\overline{Y}_2)\Theta(\overline{X}_1)/\sin \alpha_3. \qquad (A.8c)$$

In order to obtain (2.8a) and (2.8b), the expressions of the min and max functions must first be simplified. By (A.2), (A.3), (A.5) and (A.7), one finds

$$\min\,[z_1'(\overline{X}_1),z_2'(\overline{Y}_2) - r\omega_z]$$
$$= \min\,[L_{\overline{1},2} - c_1'r(\omega_y/\sin \alpha_3) - r\omega_z,$$
$$L_{\overline{1},2} - c_2'r(\omega_y \cot \alpha_3 - \omega_x)].$$

Since r tends to zero from the right, whatever $L_{\overline{1},2}$, the above quantity is equal to

$$L_{\overline{1},2} - r\max\,[c_1'(\omega_y/\sin \alpha_3) + \omega_z, c_2'(\omega_y \cot \alpha_3 - \omega_x)]$$
$$\equiv L_{\overline{1},2} - r\mathscr{W}' \qquad (A.9a)$$

and definition (2.9b) is recovered. Similarly, it is found that

$$\max\,[z_1(\overline{X}_1),z_2(\overline{Y}_2) - r\omega_z]$$
$$= r\max\,[c_1(\omega_y/\sin \alpha_3) - \omega_z,c_2(\omega_y \cot \alpha_3 - \omega_x)]$$
$$\equiv r\mathscr{W}, \qquad (A.9b)$$

which gives definition (2.9a). By these results, (A.8b) becomes

$$\mathscr{D}_{\overline{1},2} = L_{\overline{1},2} - r(\mathscr{W} + \mathscr{W}').$$

When the edge length is non-null, since $r \to 0, \mathscr{D}_{\overline{1},2}$ is always positive at sufficently small r's and the function $\Theta(\mathscr{D}_{\overline{1},2})$ can be neglected on the r.h.s. of (A.8a). However, this is not possible when the edge length is null. Therefore, depending on whether $L_{\overline{1},2} \neq 0$ or $L_{\overline{1},2} = 0$, (A.8a) can be written either as

$$\mathscr{P}_{\overline{1},2}^{(2)}(\hat{\omega},r) = e_{\overline{1},2}[L_{\overline{1},2} - r(\mathscr{W} + \mathscr{W}')] \qquad (A.10a)$$

or as

$$\mathscr{P}_{\overline{1},2}^{(2)}(\hat{\omega},r) = -e_{\overline{1},2}r(\mathscr{W} + \mathscr{W}')\Theta(-\mathscr{W} - \mathscr{W}').$$
$$(A.10b)$$

The property that the Θ-function value does not change when its argument is multiplied by a positive constant has been taken into account in order to obtain $(A.10b)$. By the same property, since $\sin \alpha_3 > 0$, $(A.8c)$ becomes

$$e_{\overline{1},2} = (\hat{\sigma}_1 \cdot \hat{\omega})(\hat{\sigma}_2 \cdot \hat{\omega})\Theta(\omega_y)$$
$$\times \Theta(\omega_y \cos \alpha_3 - \omega_x \sin \alpha_3)/\sin \alpha_3$$
$$= (\hat{\sigma}_1 \cdot \hat{\omega})(\hat{\sigma}_2 \cdot \hat{\omega})\Theta(\hat{\sigma}_1 \cdot \hat{\omega})\Theta(\hat{\sigma}_2 \cdot \hat{\omega})/\sin \alpha_3.$$
$$(A.11)$$

[In obtaining the last equality, the properties $\hat{\sigma}_1 = (0,1,0)$ and $\hat{\sigma}_2 = (-\sin \alpha_3, \cos \alpha_3, 0)$ were used. See Fig. 1.] In this way, (2.8a), (2.8b) and (2.10) are proved. Moreover, from the previous analysis, it appears clear that $(A.10a)$ holds true when r obeys the constraint $r < \min\,[L_{\overline{1},2},H_{\overline{1}},H_{\overline{2}}]$, where the $\{H_i\}$'s have been defined a few lines below $(A.4)$ Similarly, $(A.10b)$ holds true when $r < \min\,[H_{\overline{1}},H_{\overline{2}}]$. From (2.3), it follows that $\mathscr{P}^{(2)}(\hat{\omega},r)$ is a linear r function when $r < \min\,[\{\mathscr{L}'_{i,j}\},\{H_i\}]$, where $\{\mathscr{L}'_{i,j}\}$ denotes the set of edges that have a non-null length. When the facets have finite areas and the set of these values has a non-null lower bound, the previous minimum value exists and the linearity of $\mathscr{P}^{(2)}(\hat{\omega},r)$ is ensured.

References

Abramowitz, M. & Stegun, I. A. (1972). *Handbook of Mathematical Functions*, ch. 4. New York: Dover.

Benedetti, A. & Ciccariello, S. (1994). *J. Appl. Cryst.* **27**, 249–256.

Benedetti, A., Ciccariello, S. & Fagherazzi, G. (1988). *Phys. Chem. Glasses*, **29**, 173–178.

Ciccariello, S. (1990). *Acta Cryst.* A**46**, 175–186.

Ciccariello, S. (1993a). *Acta Cryst.* A**49**, 398–405.

Ciccariello, S. (1993b). *Acta Cryst.* A**49**, 750–755.

Ciccariello, S. (1993c). *J. Phys. IV (Paris)*, **3**, C8, 499–502.

Ciccariello, S. & Benedetti, A. (1982). *Phys. Rev. B*, **26**, 6384–6389.

Ciccariello, S., Cocco, G., Benedetti, A. & Enzo, S. (1981). *Phys. Rev. B*, **23**, 6474–6485.

Debye, P., Anderson, H. R. & Brumberger, H. (1957). *J. Appl. Phys.* **28**, 679–683.

Debye, P. & Bueche, A. M. (1949). *J. Appl. Phys.* **20**, 518–525.

Diez, B. & Sobry, R. (1993). *J. Phys. IV (Paris)*, **3**, C8, 511–514.

Erdélyi, A. (1956). *Asymptotic Expansions*, ch. 2. New York: Dover.

Jones, D. S. & Kline, M. (1958). *J. Math. Phys. (Cambridge, Mass.)*, **37**, 1–28.

Kirste, R. & Porod, G. (1962). *Kolloid Z.* **184**, 1–7.

Méring, J. & Tchoubar, D. (1968). *J. Appl. Cryst.* **1**, 153–165.

Porod, G. (1951). *Kolloid.* **124**, 83–87.

Porod, G. (1967). *Small Angle X-ray Scattering. Proceedings of the Syracuse Conference*, edited by H. Brumberger, pp. 1–15. New York: Gordon and Breach.

Porod, G. (1982). *Small-Angle X-ray Scattering*, edited by O. Glatter & O. Kratky, ch. 1. London: Academic Press.

Sobry, R., Fontaine, F. & Ledent, J. (1994). *J. Appl. Cryst.* **27**, 482–496.
Sobry, R., Ledent, J. & Fontaine, F. (1991). *J. Appl. Cryst.* **24**, 516–525.
Wilson, A. J. C. (1949). *X-ray Optics.* London: Methuen.

Wilson, A. J. C. (1969). *J. Appl. Cryst.* **2**, 181–183.
Wilson, A. J. C. (1970). *Elements of X-ray Crystallography*, ch. 10. Reading, MA: Addison-Wesley.
Wu, H. & Schmidt, P. W. (1971). *J. Appl. Cryst.* **4**, 224–231.
Wu, H. & Schmidt, P. W. (1974). *J. Appl. Cryst.* **7**, 131–146.

Restrained Real-Space Macromolecular Atomic Refinement using a New Resolution-Dependent Electron-Density Function

By Michael S. Chapman

Department of Biological Sciences, Purdue University, West Lafayette, Indiana 47907, USA, and Department of Chemistry* and Institute of Molecular Biophysics, Florida State University, Tallahassee, Florida 32306, USA

Abstract

A new atomic electron-density function is derived by Fourier transformation of resolution-truncated atomic scattering factors. It forms the basis of a new real-space refinement method, *RSREF*, that is a substantial improvement on prior implementations that did not formally consider the absence of high-resolution terms in a typical macromolecular electron-density map. Real-space refinement is further improved through the simultaneous refinement of stereochemical restraints analogous to reciprocal-space methods. Parallel refinements of a viral capsid structure show that real-space refinement produces models that are at least as good as those refined in reciprocal space, by either restrained or molecular-dynamics methods, and that refinement cycles are $\sim$50 times faster. Real-space refinement will not replace reciprocal-space methods for proteins, where, without the high noncrystallographic symmetry of viruses, experimental phases and electron-density maps are not of the same high quality. However, applied to local regions, it can be used to speed up and improve the quality of interactive model building before a full refinement is started.

1. Notation

a	Atomic radius
A, B	Real and imaginary parts of a structure factor
B	Temperature factor
d^*	Reciprocal-space distance from origin
d^*_{min}, d^*_{max}	Reciprocal-space resolution limits
F^{obs}, F^{calc}	Observed and calculated structure factors
f	Form factor
g	Scattering factor with thermal motion, $g = f(d^*)\exp(-Bd^{*2}/4)$
G	Fourier transform of a solid sphere
h^*	Reciprocal-space distance
h	Reflection index
H	Total number of reflections
k	Scaling constant (reciprocal space) or threshold (real space)
M	Number of atoms
$\mathcal{R}$	Overall residual minimized in least squares
$\mathcal{R}_{geom}$	Residual difference between model and ideal stereochemistry
$\mathcal{R}_\rho$	Residual difference between observed and calculated electron density
$\mathcal{R}_{\text{X-ray}}$	Residual difference between observed and calculated structure factors
R^{conv}	Conventional reciprocal-space R factor
$R^{\mathcal{ED}}$	Real-space R factor
R^{free}_T	Reciprocal-space free R factor (Brünger, 1992)
r	Radial distance from the center of an atom
r^{max}_{calc}	Maximum r for calculation of electron density
r^{max}_{ref}	Maximum r for calculation of derivatives
ρ_m	Electron density for the mth atom
ρ_c	Electron density calculated from all atoms of a model
ρ_o	Observed electron density
S	Scale constant to bring ρ_o to an absolute scale
T	Generic Fourier transform
w	Figure of merit
Z	Number of electrons in an atom

---

* Current address.

2. Introduction

Although real-space methods of refinement were applied successfully to some of the first protein structures (Diamond, 1974; Deisenhofer & Steigemann, 1975;